Talanta 133 (2015) 27–33

Contents lists available at ScienceDirect

Talanta

journal homepage: www.elsevier.com/locate/talanta

Visual detection and sequential injection determination of aluminium using a cinnamoyl derivative

Lenka Elečková [a,*], Michal Alexovič [a], Juraj Kuchár [b], Ioseph S. Balogh [c], Vasil Andruch [a]

[a] Department of Analytical Chemistry, P.J. Šafárik University, SK-04154 Košice, Slovak Republic
[b] Department of Inorganic Chemistry, P.J. Šafárik University, SK-04154 Košice, Slovak Republic
[c] Department of Chemistry, College of Nyíregyháza, HU-4400 Nyíregyháza, Hungary

ARTICLE INFO

Article history:
Received 24 September 2013
Received in revised form
8 April 2014
Accepted 22 April 2014
Available online 30 April 2014

Keywords:
Aluminium
Visual detection
Sequential injection analysis
Ligand

ABSTRACT

A cinnamoyl derivative, 3–[4–(dimethylamino)cinnamoyl]–4–hydroxy–6–methyl–3,4–2*H*–pyran–2–one, was used as a ligand for the determination of aluminium. Upon the addition of an acetonitrile solution of the ligand to an aqueous solution containing Al(III) and a buffer solution at pH 8, a marked change in colour from yellow to orange is observed. The colour intensity is proportional to the concentration of Al (III); thus, the 'naked–eye' detection of aluminium is possible. The reaction is also applied for sequential injection determination of aluminium. Beer's law is obeyed in the range from 0.055 to 0.66 mg L^{-1} of Al (III). The limit of detection, calculated as three times the standard deviation of the blank test ($n=10$), was found to be 4 μg L^{-1} for Al(III). The method was applied for the determination of aluminium in spiked water samples and pharmaceutical preparations.

© 2014 Elsevier B.V. All rights reserved.

1. Introduction

Aluminium is a widespread metal occurring naturally in bauxite rock, silicates and cryolite. Its path into drinking water and food occurs through a transmission chain in nature caused primarily by human activity [1]. Aluminium and its compounds have extensive applications in a variety of fields, mainly in the manufacture of alloys, glass and ceramics and in the automobile and transport industries. It is also used in cosmetics production and the pharmaceutical and food industries [1,2]. Aluminium salts are used as coagulants for the treatment of drinking water. According to WHO, the tolerable value of aluminium in drinking water is limited to 0.2 mg L^{-1} [3]. The continuous increase in human activity leads to soil acidification and thus contributes to higher levels of mobile forms of aluminium. Hartwell and Pember [4], in 1918 studied the toxic effect of aluminium on plants due to increasing acidity in the soil substrate, and thus far several studies have been published on this topic [5–7]. The effect of aluminium on the human body and human health as well as aluminium intake through cosmetic preparations [8] and pharmaceutical preparations [9–11], particularly in childhood vaccines [12–14], is still being discussed. Aluminium has a potential neurotoxic effect [15], and its intake by the human organism is connected with, for example, Alzheimer's disease [16–19], autism [20] and breast cancer [8]. Therefore, the determination of aluminium in environmental, pharmaceutical and cosmetic preparations is very important and greatly needed [21].

Several articles concerning the determination of aluminium using flow analysis and atomic spectrometry [22], fluorimetry [23,24], or spectrophotometry [25–27] have been published. Developing visual detection procedures can be considered as one of the most interesting topics in analytical chemistry today. Several articles on the visual detection of a variety of cations and anions [28–33], including aluminium, have been published (Table 1).

In this work, the reaction of Al(III) with 3–[4–(dimethylamino) cinnamoyl]–4–hydroxy–6–methyl–2*H*–pyran–2–one ligand (L) was employed (Fig. 1) for the visual detection and sequential injection determination of aluminium. The ligand is a cinnamoyl derivative belonging to the family of cinnamoyl pyrones. Cinnamoyl pyrones are known as medicaments and as intermediate products of medicament synthesis [34]. The structure and spectral properties of cinnamoyl pyrones were discussed by Tykhanov et al. [34,35].

Abbreviations: L, 3–[4–(dimethylamino)cinnamoyl]–4–hydroxy–6–methyl–2 *H*–pyran–2–one (ligand); SV, Selection Valve; HC, Holding Coil; RC, Reaction Chamber; SP, Syringe Pump; B, Buffer solution; A, Acetone; AN, Acetonitrile; SVo, Sample Volume; LR, Linear Range; BR, Bromopyrogallol Red; n–TCTMAB, n–Tetradecyltrimethylammonium bromide; CAS, Chromeazurol S; CPC, Cetylpyridiniumchloride; ARS, Alizarin Red S; PV, Pyrocatechol Violet; MTB, Methyl Thymol Blue; A DBM, Arsenazo DBM; ECR, Eriochrome cyanine R; CTMAB, Cetyltrimethylammonium bromide; AQ, Anthraquinones.

* Corresponding author. Tel.: +421 55 234 2323.
E-mail address: lenka.eleckova@gmail.com (L. Elečková).

http://dx.doi.org/10.1016/j.talanta.2014.04.064
0039-9140/© 2014 Elsevier B.V. All rights reserved.

Table 1
Comparison of the developed visual method of Al(III) with those previously published in the literature.

Ligand	Comments	Sample	CC	LOD	Ref.
3–[4–(Dimethylamino)cinnamoyl]–4–hydroxy–6–methyl–2*H*–pyran–2–one	Water:AN (4.3:0.7, v/v); pH 8.0; SIA UV–vis detection (*CC*: up to 0.66 mg L^{-1}, *LOD*: 4 μg L^{-1})	Tap and spring water	0.11–0.88 mg L^{-1}	0.11 mg L^{-1}	This work
5–[(2–Hydroxy–5–nitro–benzylidene)–amino]–1 *H*–pyrimidine–2,4–dione	DMSO:water (95:5, v/v)	–	–	25–50 μmol L^{-1}	[36]
2–(2–(2–Hydroxyethoxy)ethoxy)ethyl 8–propoxyquinoline–2–carboxylate	AN:water (95:5, v/v)	Tap water	0–23 μmol L^{-1}	0.8 μmol L^{-1}	[37]
5–[{(2–Hydroxynaphthalen–1–yl) methylene}amino]pyrmidine–2,4 (1*H*,3*H*)–dione	UV–vis detection (*CC:* up to 50 μmol L^{-1} in AN) Fluorescent detection (*CC:* 0–2 equiv Al^{3+}; *LOD:* 3.2×10^{-7} mol L^{-1} in AN, 1×10^{-6} mol L^{-1} in water)	–	–	–	[38]
Under UV-light					
2,2′–Dihydroxyazobenzene	Spot test on hydrophobic filter paper; pH 6.5	–	–	2×10^{-8}mol L^{-1}	[39]
2,2′–Dihydroxyazobenzene	The hydrophobic surface of the octadecylsilanized silica thin layer	Tap and river water, tea	–	1 μg L^{-1}	[40]
4–(8′–Hydroxyquinolin–5′–yl) methyleneimino–1–phenyl–2,3–dimethyl–5–pyzole	10% methanol solution; pH 4.5; Fluorescent detection (*CC:* 0–22 μmol L^{-1}; *LOD*: under 10^{-7} mol L^{-1})	–	–	–	[41]
2–Hydroxynaphthylidene– (8′–aminoquinoline)	DMF solution; Fluorescent detection (*CC:* 0–16 equiv Al^{3+}; *LOD:* 1 μmol L^{-1})	–	–	–	[42]
Methyl pyrazinylketone benzoyl hydrazone	Ethanol solution; Fluorescent detection (*CC:* 0–1 equiv Al^{3+}; *LOD:* 10^{-7} mol L^{-1})	–	–	–	[43]

CC, Calibration curve; AN, Acetonitrile; –, data not found in paper.

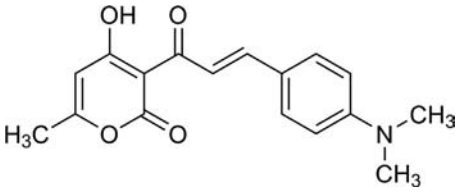

Fig. 1. Structure of 3–[4–(dimethylamino)cinnamoyl]–4–hydroxyl–6–methyl–2*H*–pyran–2–one.

To the best of our knowledge, there have been no publications on the application of this ligand to the spectrophotometric determination of analytes.

2. Experimental

2.1. Reagents

All reagents and solvents were of analytical grade purity. Distilled water was used throughout the experiment. A stock aqueous solution containing 10 mmol L^{-1} of Al(III) was prepared by dissolving 0.1876 g of $Al(NO_3)_3 \cdot 9H_2O$ (Centralchem, Slovakia) in water and diluting to 50 mL. The working solutions of various concentrations of Al(III) were prepared by step-wise dilution of the stock solution. The 1 mmol L^{-1} solution of ligand was prepared by dissolving 0.0299 g of 3–[4–(dimethylamino)cinnamoyl)]–4–hydroxy–6–methyl–2*H*–pyran–2–one in 100 mL of acetonitrile (Merck, Germany). The pH of the aqueous phase was adjusted by the addition of CH_3COOH–NH_4OH buffer solutions, which were prepared by mixing equimolar solutions (1 mol L^{-1}) of CH_3COOH and NH_4OH (both Centralchem, Slovakia) in various ratios (v/v). The buffer solution with pH 8 was prepared in ratio of 24.65:25.35 (CH_3COOH:NH_4OH, v/v).

2.2. Apparatus

A Lightwave II UV–vis spectrophotometer (Biochrom Ltd., United Kingdom) and a Specord S 600 diode-array spectrophotometer (Analytik Jena AG, Germany) equipped with matched quartz cells of 10 mm path length were used for UV–vis spectrophotometric measurements. The pH values were measured using an ORION 720A$^+$ pH metre with a glass electrode. The ATR measurement technique was performed on a Nicolet 6700 FT–IR spectrometer (Thermo Fisher Scientific Inc., USA).

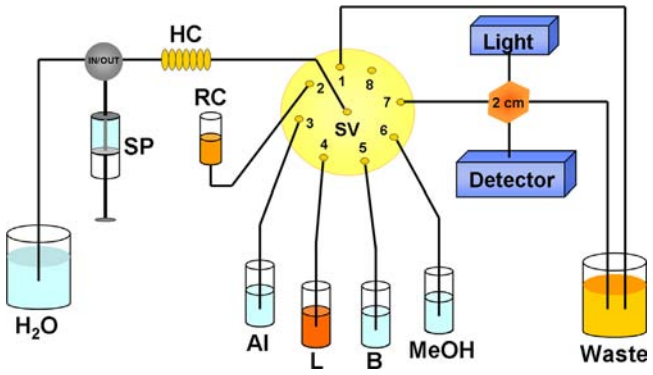

Fig. 2. The suggested set-up of sequential injection manifold. **SP**, syringe pump; **HC**, holding coil; **RC**, reaction chamber; **SV**, selection valve; **L**, ligand; **B**, buffer solution.

The sequential injection manifold (Fig. 2) is based on the commercially available FIAlab® 3500 system (FIAlab® Instrument Systems Inc., Bellevue, USA) and equipped with a glass syringe pump (SP) (5 mL) and a central eight-port Cheminert selection valve (Valco Instrument Co., Houston, USA). The central port of the selection valve (SV) was connected to a holding coil (HC), and the lateral ports of the SV were connected as follows: waste (port 1), *reaction chamber* (RC – a 2 mL microcentrifuge polypropropylene tube with a snap-on cap and 1.2 cm of i.d. width) (port 2), sample (Al) (port 3), ligand (port 4), buffer solution with pH 8 (port 5), methanol (port 6), air (port 8). Port 7 was directed to an optical *Z*-flow cell (20 mm) and flowed into a waste receptacle. An LS-1-LL tungsten halogen lamp (Ocean Optics Inc., Dunedin, USA) was used as the light source and the CCD USB 2000 diode array spectrophotometer (Ocean Optics Inc., Dunedin, USA) as the detector. FIAlab® software (version 5.9.321) served as the operating programme, enabling the control of the flow procedure and the acquisition and evaluation of data.

2.3. General procedure for visual and spectroscopy study

Aqueous solutions containing Al(III) from 0.055 to 0.66 mg L^{-1} were put into test tubes, and 1 mL of buffer solution was added. The volume was then filled up to 4.3 mL with water, and 0.7 mL of the 1 mmol L^{-1} acetonitrile solution of ligand was added to achieve final volume of 5 mL. The solution was mixed thoroughly after the addition of each reagent, especially during the last addition.

2.4. Operational protocol for sequential injection analysis

The entire procedure started with the aspiration of water from the reservoir (1500 μL, 1000 μL s^{-1}) into the SP. The reagents were then aspirated into HC at 35 μL s^{-1} in this order: sample (80 μL), buffer solution pH 8 (80 μL) and the ligand (80 μL). Afterwards, the volume of 240 μL containing all reagents was injected into the RC, which was refilled with water up to 400 μL (40 μL s^{-1}) in order to achieve the final volume of the solution. The solution was then intensively mixed by air bubbling (800 μL, 800 μL s^{-1}). After a delay of 30 s, which proved to be sufficient time for complex formation between Al(III) and the ligand, the 100 μL of the aqueous solution was aspirated back into the HC at 30 μL s^{-1} flow-rate and pushed to waste in order to fulfil tube connecting port 2 with RC and avoiding any occurence of bubbles inside the HC. In the next step, the volume of 65 μL (30 μL s^{-1}) of aqueous solution was aspirated to HC once again and immediately propelled (450 μL at 40 μL s^{-1}) toward the *Z*-flow cell for UV–vis spectrophotometric detection at 520 nm wavelength. In the final step, the HC and the RC were twice cleaned using methanol–water mixture. The determination of aluminium was accomplished in less than 220 s.

3. Results and discussion

3.1. Visual detection and UV–vis spectrophotometric study

Upon the addition of an acetonitrile solution of the ligand to an aqueous solution containing Al(III) and a buffer solution at pH 8, a marked change in colour from yellow to orange is observed. The change in the colour intensity is proportional to the increasing concentration of Al(III). Thus, the 'naked–eye' detection of aluminium was easily observable (Fig. 3A). Other ions, such as Na(I), K(I), Mg(II), Ca(II), Cr(VI), Mn(II), Co(II), Ni(II), Zn(II), Ag(I), Cd(II), and Pb(II), did not exhibit any detectable colour change in the absence of Al(III) (Fig. 3B). By testing of standard solution containing Fe(III) ion, a minor colour change was observed in comparison with blank (Fig. 3B). Therefore masking of Fe(III) with CN^- ions was carried out. According to obtained results, Fe(III) in the presence of CN^- provided the same colour as other above mentioned cations in the absence of Al(III), thus no interference was observed at this stage. The selectivity is tested in more detail in the *SIA procedure section*. Visual detection was applied in different water samples (tap water and spring water), spiked with known amount of aluminium. From the Fig. 3C it is obvious, that in all cases, same colour changes were observed.

The interaction between the ligand and Al(III) was confirmed using UV–vis spectrophotometry upon the addition of an acetonitrile solution of the ligand to an aqueous solution containing various amounts of Al(III) at pH 8, while the ligand concentration was kept constant in all experiments. The ligand exhibited its primary absorption peak at 407 nm (Fig. 4). Upon addition of an increasing amount of Al(III), the peak at 407 nm gradually decreased and a new absorption band gradually appeared at 515–545 nm. The distinct isosbestic point at 448 nm indicates the formation of the complex of Al(III) with ligand. From the results obtained, the calibration plot was constructed at 520 nm (Fig. 4).

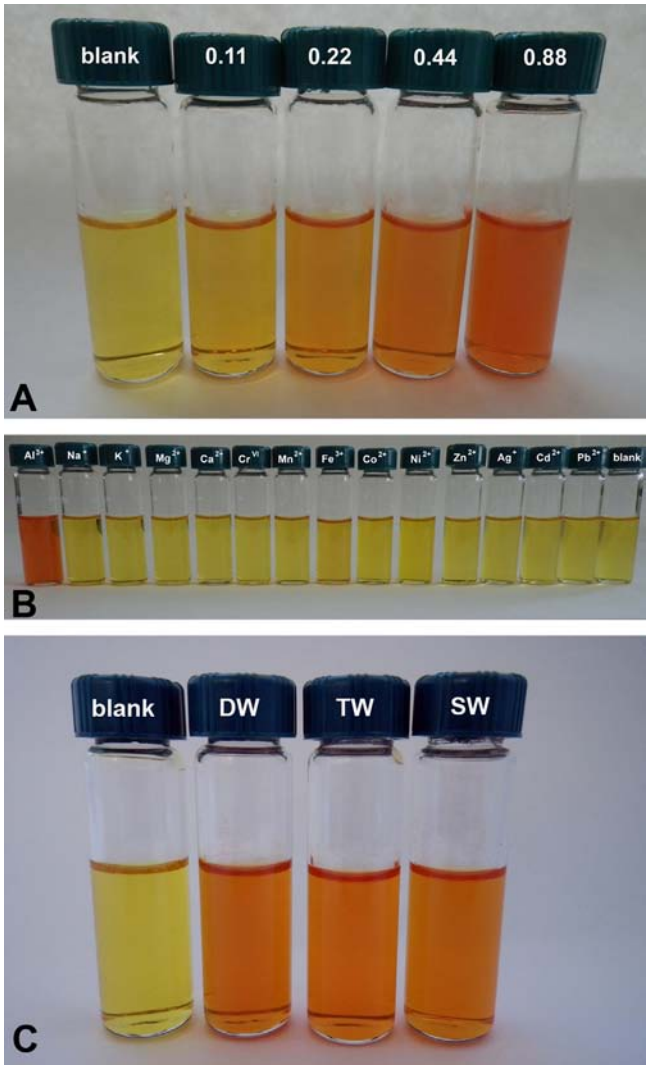

Fig. 3. Pictures illustrated the colour changes. The final conditions: 0.14 mmol L^{-1} of ligand, pH 8, ratio of water:acetonitrile (4.3:0.7 v/v). (A) Colour changes of the ligand proportional to various concentration levels of Al(III), from 0.11 to 0.88 mg L^{-1} (from 4 to 32 μmol L^{-1}); (*B*) Comparison of colour changes of the ligand in the presence of 0.1 mmol L^{-1} of Al(III) to 0.1 mmol L^{-1} of other metal ions; (*C*) Visual detection of Al(III) in different spiked water samples (DW – Distilled water, TW – Tap water, SW – Spring water) at 0.44 mg L^{-1} (16 μmol L^{-1}) of Al(III). (For interpretation of the references to colour in this figure legend,the reader is referred to the web version of this article)

3.2. Reaction kinetic study

Due to the low water solubility of the ligand its solubility in various water-miscible solvents such as methanol, ethanol, 2–propanol, acetone and acetonitrile was investigated. The best solvents seem to be acetonitrile and acetone.

The reaction kinetics of the ligand dissolved in acetonitrile, acetone and in mixtures of acetonitrile and acetone at various v/v ratios and Al(III) were investigated for 1 h by means of UV–vis spectrophotometry. The experimental conditions are described in the *General procedure section*. A part of this reaction course is shown in Fig. 5. The analytical response shows more rapid growth and reaches a maximum value much faster in the case of acetonitrile (4 min) compared with acetone (20 min). However, the signal stability is better in the case of acetone. Therefore, we

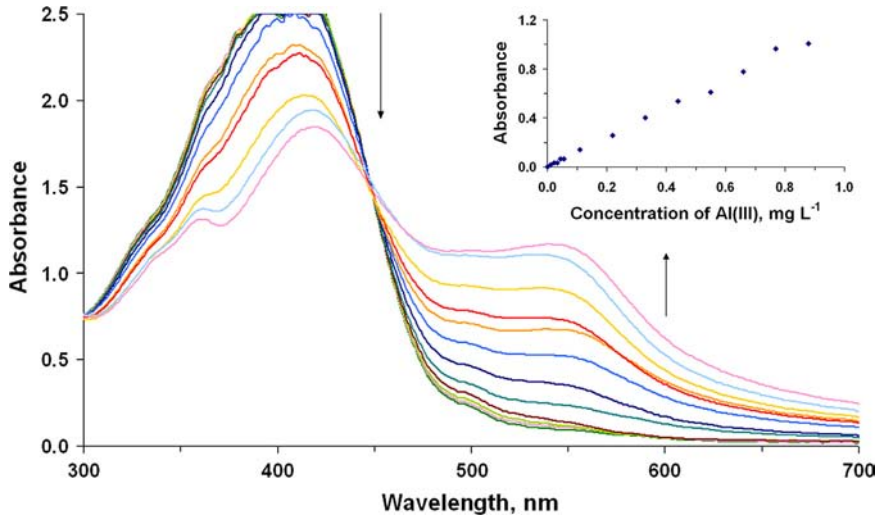

Fig. 4. UV–vis spectra of 0.14 mmol L^{-1} of ligand in water–acetonitrile (4.3:0.7 v/v) solution at pH 8 with increasing concentrations of Al(III); $l=1$ cm and calibration curve (inset graph) measured at 520 nm.

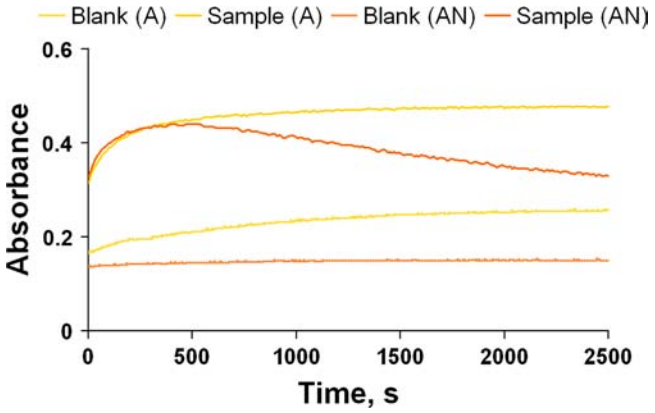

Fig. 5. Kinetic study of complex formation between Al(III) and the ligand dissolved in (*A*) acetone and (AN) acetonitrile pH 8; 0.14 mmol L^{-1} of ligand; $l=1$ cm; $\lambda=520$ nm.

investigated a mixture of acetone and acetonitrile in different v/v ratios. We can note some advantages of using this mixture: for example, the analytical response reaches a maximum value faster when compared with acetone, and the signal stability in time is better comparing with acetonitrile. However, due to the lower value of the blank test and better repeatability, acetonitrile was chosen as the most appropriate for subsequent experiments.

3.3. IR spectroscopic study

The composition of the ligand and the Al(III)–ligand complex in the solid state was verified using the IR technique (ATR). Absorption bands were identified and assigned according to the literature [44,45]. As expected, the spectrum is rather complex due to the low symmetry of the ligand. On the other hand, we did not expect any strong intermolecular interaction, so the assignment in the solid state can be performed as though with an unperturbed molecule. The main features are at 1730 cm^{-1} and 1653 cm^{-1}, and the absorption bands belong to C=O stretching vibration of the carbonyl groups. The localised C=C bond in the structure was identified by the absorption band at 1593 cm^{-1}, and in the region from 1540 cm^{-1} to 1450 cm^{-1} the absorption bands were assigned to the stretching vibration of C–C from the aromatic ring accompanied by the stretching vibration of C–N and C–C bonds. Unfortunately, the precise assignment of the absorption bands is complicated, and without the use of other techniques (e.g. isotopic exchange) it is unreasonable. The aromatic ring can also be identified by the weak absorption bands at 3099 cm^{-1} and 3078 cm^{-1}, which belong to stretching vibration of the C–H bonds. The methyl group can be identified by the symmetrical and unsymmetrical deformation vibration that is evidenced by the weak bands at 2914 cm^{-1} and 2829 cm^{-1}, which belong to the stretching vibration of the C–H bonds. All other absorption bands were difficult to identify and therefore no further analysis was performed.

The IR technique was also used to verify the formation of the aluminium atom bond to the oxygen atom in the formed complex. The complex of the ligand with Al(III) was prepared from 64 mg of $Al(NO_3)_3 \cdot 9H_2O$ dissolved in 3 mL of distilled water and 153 mg of the ligand dissolved in 1.5 mL of methanol. The mixture was refluxed for 3 h before being filtered and dried. As is mentioned in the literature [46], the coordination of the oxygen atom from the carbonyl group leads to a lowering of the frequency of the stretching vibration. In our case, the absorption band that was before found at 1730 cm^{-1} (as mentioned above) not only shifted to 1723 cm^{-1}, but its shape changed and a shoulder appeared at 1716 cm^{-1}. As expected, no other bands shifted; they remained more or less in the same position (Fig. 6).

3.4. SIA procedure

3.4.1. Optimisation of the SIA procedure

In order to find the appropriate experimental conditions, the effect of the following variables was investigated: pH, concentration of ligand, flow rate, aspiration sequence, and reaction time. The highest analytical signal at the lowest value of blank and the lowest relative standard deviation was chosen as the main criterion. From Fig. 7 it is obvious that the maximum complexation of Al(III) with the ligand is reached at pH 8 and a ligand concentration equal to 0.2 mmol L^{-1}.

The various volumes of reagents in a range 40–100 μL, the flow rate in a range 10–100 μL s^{-1} and different aspiration sequences of reagents were also studied. The following aspiration sequences were tested: Al–pH–L, Al–L–pH, pH–Al–L, pH–L–Al, L–pH–Al, L–Al–pH (80 μL for all reagents), pH–Al–L–pH, Al–pH–L–pH; L–pH–Al–pH (40 or 50 μL for each pH segment and 80 μL for the other reagents), pH–L–pH–Al–pH (30 μL for each pH segment and 80 μL for the other reagents). The best result was obtained in the case of aspiration sequence Al–pH–L, 80 μL volume of all reagents at a

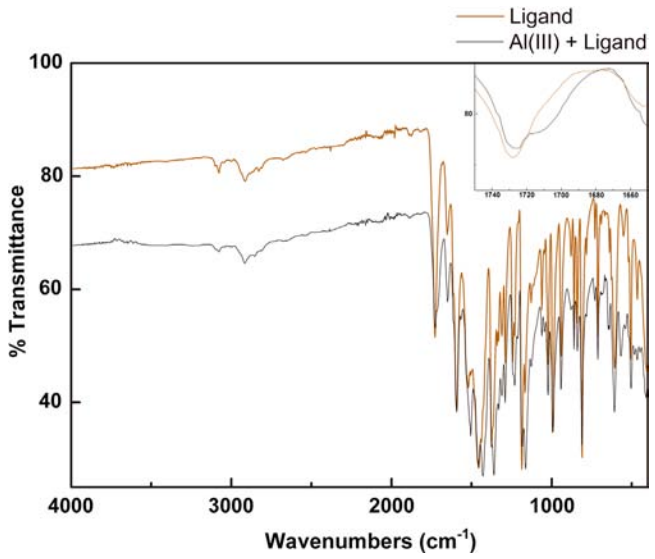

Fig. 6. IR spectra.

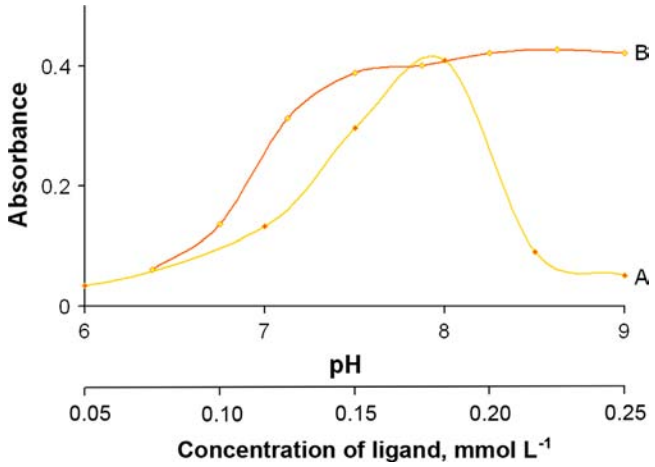

Fig. 7. Effect of pH (*A*), and concentration of ligand (*B*). Experiments at optimal conditions: 0.33 mg L^{-1} Al(III); $l=2$ cm; $\lambda=520$ nm. (A) 0.2 mmol L^{-1} of ligand, (B) pH 8.

flow rate of 35 μL s^{-1} and mixing using 800 μL air at a flow rate of 800 μL s^{-1}. Finally, the reaction time (the time between mixing of the sample and all necessary reagents in the RC and the detection step) required for complex forming of Al(III) with the ligand in range 0–300 s was tested. The analytical response increases up to 30 s and does not change with further increase in reaction time. Thus, in order to reduce the time for analytical assay, a reaction time of 30 s was chosen for further experiments.

3.4.2. Figures of merit

A calibration plot was constructed in the range from 0.055 to 0.66 mg L^{-1} at seven concentration levels. The regression equation was $A=0.1627\times C+0.0131$, where A is the absorbance and C is the concentration of aluminium in mg L^{-1}. The limit of detection (LOD), calculated as three times the standard deviation of the blank test ($n=10$), was found to be 4 μg L^{-1} of Al(III). The precision and accuracy of the developed method were checked by performing five replicate determinations of aluminium at two concentration levels on three different days and then calculated as the relative standard deviation percentage (RSD, %) and the recovery percentage (R, %). The precision and accuracy results

Table 2
Inter-day precision and accuracy data for the determination of aluminium, $n=5$.

Realized	Taken (mg L^{-1})	Determined[a] (mg L^{-1})	RSD (%)	R (%)
1st day	0.28	0.29 ± 0.01	2.8	103.6
	0.50	0.49 ± 0.01	1.6	98.0
2nd day	0.28	0.27 ± 0.01	3.0	96.4
	0.50	0.51 ± 0.01	1.6	102.0
3rd day	0.28	0.28 ± 0.01	2.9	100.0
	0.50	0.49 ± 0.01	1.6	98.0

[a] $\bar{x}\pm s\ (t/\sqrt{n})$ ($t=2.776$, $P=0.95$), t-student coefficient for n–1 degrees of freedom; RSD – Relative standard deviation percentage; R – Recovery percentage.

Table 3
Application of the suggested method to the determination of aluminium in spiked and real samples.

Sample	[a]Added (mg L^{-1})/ [b]Declared	[d]Found (mg L^{-1})	RSD (%)	R (%)
Tap water	–	–	–	–
	[a]0.22	0.22 ± 0.01	3.7	100.0
	[a]0.55	0.56 ± 0.02	2.9	101.8
Spring water	–	–	–	–
	[a]0.22	0.23 ± 0.01	3.5	104.5
	[a]0.55	0.55 ± 0.03	4.4	100.0
Antacid suspension	[b,c]382 mg/5 mL	[e]370.7 ± 15.6 mg/ 5 mL	3.4	97.0
Antiperspirant solution	[b,c]185 mg mL^{-1}	[e]184.7 ± 6.8 mg mL^{-1}	3.0	99.8

[a] Amount of Al(III) added to the sample.
[b] Declared amount of aluminium compound contained in preparation.
[c] Content of aluminium compound in preparation.
[d] $\bar{x}\pm s\ (t/\sqrt{n})$ ($t=2.776$, $P=0.95$), t-student coefficient for n–1 degrees of freedom; RSD – Relative standard deviation percentage; R – Recovery percentage.
[e] Calculated as content of aluminium compound in preparation.

are presented in Table 2; they show the good repeatability of the suggested method.

The effect of some interfering ions on the determination of 0.22 mg L^{-1} of Al(III) was also examined. A molar ratio of Al(III): interfering ion which resulted in an error not exceeding ±5% was taken as the tolerable amount. Among cations, a more than 5,000–fold excess of Na(I) and K(I), a 250–fold excess of Mg(II), a 150–fold excess of Ca(II), a 50–fold excess of Cr(VI) and Ag(I), a 25–fold excess of Co(II), a 20–fold excess of Mn(II), a 10–fold excess of Ni (II), Cd(II) and Zn(II) and a 10–fold excess of Fe(III) after masking with CN^- ions did not interfere the determination of aluminium. With anions a 5,000–fold excess of Cl^-, I^-, SO_4^{2-} and a 1,000–fold excess of $S_2O_3^{2-}$ and HCO_3^- showed no interference with the determination of aluminium.

3.4.3. Analysis of real samples

The applicability of the developed SIA procedure was tested as a study of precision and accuracy of the determination of aluminium in water samples after standard addition. The recovery study shows that added aluminium can be quantitatively recovered from water samples. The method was also applied to the determination of aluminium in pharmaceutical preparations. An antiperspirant solution containing 185 mg/mL of $AlCl_3\times6H_2O$ and an antacid suspension containing 382 mg/5 mL of $Al(OH)_3$ were used as pharmaceutical samples. In order to obtain a clear solution of antacid from the suspension form, 1 mol L^{-1} HCl was used. Before analysis, the real samples were diluted with water to reach a concentration of Al(III) located within the linear working range.

Table 4
Comparison of the developed SIA method with those previously published in the literature for on-line determination of Al(III) using UV–vis detection.

Ligand	Sample	SVo (μL)	λ (nm)	LR (mg L^{-1})	LOD (μg L^{-1})	Refs.
BR/n–TCTMAB	River water	160	623	Up to 0.1 Up to 0.3	1	[47]
CAS/CPC	Tap water	120	625	Up to 0.4	5	[48]
PV	Potable and treated water	–	580	Up to 1	45	[49]
ARS	Kaolin	75	510	Up to 25	800	[50]
CAS/CPC	River water	–	625	Up to 1.13	18	[51]
PV	River, tap water	280	580	0.01-0.08	5	[52]
MTB	Silicate materials and ores	200	528	0.25–2	30	[53]
A DBM	Steel	–	613	3–18	1500	[54]
ECR	Antiperspirant	50	535	0.15–0.9	16.1	[25]
Quercetin/CTMAB	Tap water	–	428	0.02–0.5	7	[26]
AQ	Tea	75	499	0.1–1	50	[27]
L	Water, pharmaceuticals	80	520	0.055–0.66	4	This work

SVo, Sample volume; LR, Linear range; BR, Bromopyrogallol Red; n-TCTMAB, n-Tetradecyltrimethylammonium bromide; CAS, Chromeazurol S; CPC, Cetylpyridiniumchloride; ARS, Alizarin Red S; PV, Pyrocatechol Violet ; MTB, Methyl Thymol Blue; A DBM, Arsenazo DBM; ECR, Eriochrome cyanine R; CTMAB, Cetyltrimethylammonium bromide; AQ, Anthraquinones; L, 3–[4–(Dimethylamino)cinnamoyl]–4–hydroxy–6–methyl–2*H*–pyran–2–one.

For adjustment of neutral pH, 1 mol L^{-1} NH_4OH was used. The results are shown in Table 3.

4. Conclusion

The reaction of Al(III) with the ligand 3–[4–(dimethylamino) cinnamoyl]–4–hydroxy–6–methyl–2*H*–pyran–2–one was employed for novel and simple methods of visual detection and sequential injection determination of aluminium. The suggested visual method, in comparison with previous published in the literature: (1) presents visual calibration in the range 0.11–0.88 mg L^{-1}; (2) is suitable for aqueous samples, as only the ligand must be dissolved in acetonitrile; and (3) was applied to the determination of aluminium in real samples. Table 4 shows a comparison of the suggested SIA method with previous flow-based methods published in the literature for on-line determination of Al(III) using UV–vis detection. The suggested SIA method: (1) gives a better LOD value [25–27,48–54]; (2) requires a smaller amount of sample [47,48,52,53]; and (3) unlike previous methods, requires no adding of a surfactant [26,47,48,51]. The SIA procedure was applied to the determination of aluminium in spiked water samples and pharmaceutical preparations.

Acknowledgements

The authors express their gratitude to the scientific Grant Agency of the Ministry of Education of the Slovak Republic and the Slovak Academy of Sciences (VEGA 1/1096/12).

References

[1] D. Krewski, R.A. Yokel, E. Nieboer, D. Borchelt, J. Cohen, J. Harry, S. Kacew, J. Lindsay, A.M. Mahfouz, V. Rondeau, Crit. Rev. 10 (2007) 1–269.
[2] R.A. Yokel, Aluminum in food – the nature and contribution of food additives, in: Y. El–Samgary (Ed.), Food Additive, InTech for Europe, Croatia, 2012, pp. 203–228.
[3] WHO, Aluminium, Guidelines for Drinking-Water Quality, 4th ed., World Health Organization, Geneva, 2011.
[4] B.L. Hartwell, F.R. Pember, Soil. Sci. 6 (1918) 259–277.
[5] M. Schaedele, F.C. Thornton, D.J. Raynal, H.B. Tepper, Tree Physiol. 5 (1989) 337–356.
[6] J. Furukawa, N. Yamaji, H. Wang, N. Mitani, Y. Murata, K. Sato, M. Katsuhara, K. Takeda, J.F. Ma, Plant Cell Physiol. 48 (2007) 1081–1091.
[7] L.G. Maron, C.T. Guimarães, M. Kirst, P.S. Albert, J.A. Birchler, P.J. Bradbury, E.S. Buckler, A.E. Coluccio, T.V. Danilova, D. Kudrna, J.V. Magalhaes, M. A. Piñeros, M.C. Schatz, R.A. Wing, L.V. Kochian, Proc. Natl. Acad. Sci. 110 (2013) 5241–5246.
[8] P.D. Darbre, J. Inorg. Biochem. 99 (2005) 1912–1919.
[9] S. Zaręba, J. Melke, Pharm. Acta Helv. 74 (2000) 361–364.
[10] D.G. Themelis, F.S. Kika, J. Pharm. Biomed. Anal. 41 (2006) 1179–1185.
[11] J. Komárek, R. Červenka, T. Ružička, V. Kubáň, J. Pharm. Biomed. Anal. 45 (2007) 504–509.
[12] E.B. Lindblad, Vaccine 22 (2004) 3658–3668.
[13] J.M. Brewer, Immunol. Lett. 102 (2006) 10–15.
[14] L. Tomljenovic, C.A. Shaw, Curr. Med. Chem. 18 (2011) 2630–2637.
[15] V. Kumar, K.D. Gill, Arch. Toxicol. 83 (2009) 965–978.
[16] V.B. Gupta, S. Anitha, M.L. Hegde, L. Zecca, R.M. Garruto, R. Ravid, S.K. Shankar, R. Stein, P. Shanmugavelu, K.S. Jagannatha Rao, Cell. Mol. Life Sci. 62 (2005) 143–158.
[17] L. Tomljenovic, J. Alzheimers Dis. 23 (2011) 567–598.
[18] S. Davenward, P. Bentham, J. Wright, P. Crome, D. Job, A. Polwart, C. Exley, J. Alzheimers Dis. 33 (2013) 423–430.
[19] P. De Sole, C. Rossi, M. Chiarpotto, G. Ciasca, B. Bocca, A. Alimonti, A. Bizzarro, C. Rossi, C. Masullo, Clin. Biochem. 46 (2013) 89–93.
[20] S. Seneff, R.M. Davidson, J. Liu, Entropy 14 (2012) 2227–2253.
[21] R.A. Yokel, P.J. McNamara, Pharm. Toxicol. 88 (2001) 159–167.
[22] H.J. Salacinski, Anal.Chim. Acta 269 (1992) 1–7.
[23] G.d.e. Armas, M. Miró, A. Cladera, J.M. Estela, V. Cerdà, Anal. Chim. Acta 455 (2002) 149–157.
[24] C. Brach – Papa, B. Coulomb, J.L. Boudenne, V. Cerdà, F. Theraulaz, Anal. Chim. Acta 457 (2002) 311–318.
[25] A. López – Gonzálvez, M. A., C. Barbas, J. Pharm. Biomed. Anal. 48 (2008) 340–346.
[26] P. Norfun, T. Pojanakaroon, S. Liawraungrath, Talanta 82 (2010) 202–207.
[27] S. Tontrong, S. Khonyoung, J. Jakmunee, Food Chem. 132 (2012) 624–629.
[28] Q. Mei, L. Wang, B. Tian, F. Yan, B. Zhang, W. Huang, B. Tong, New J. Chem. 36 (2012) 1879–1883.
[29] Y. Yu, W. Dou, X. Hu, X. Tang, X. Zhou, W. Liu, J. Fluoresc. 22 (2012) 1547–1553.
[30] W.T. Gong, B. Gao, S. Bao, J.W. Ye, G.L. Ning, J. Incl. Phenom. Macrocycl. Chem. 72 (2012) 481–486.
[31] Y. Wang, L. Wang, L.L. Shi, Z.B. Shang, Z. Zhang, W.J. Jin, Talanta 94 (2012) 172–177.
[32] X. Liu, H.T. Ngo, Z. Ge, S.J. Butler, K.A. Jolliffe, Chem. Sci. 4 (2013) 1680–1686.
[33] Q. Lin, Y.P. Fu, P. Chen, T.B. Wei, Y.M. Zhang, Dyes Pigments 96 (2013) 1–6.
[34] D.O. Tykhanov, E.V. Sanin, I.I. Serikova, F.G. Yaremenko, A.D. Roshal, Spectrochim. Acta A 83 (2011) 221–230.
[35] D.A. Tykhanov, I.I. Serikova, F.G. Yaremenko, A.D. Roshal, Cent. Eur. J. Chem. 8 (2010) 347–355.
[36] K.K. Upadhyay, A. Kumar, Talanta 82 (2010) 845–849.
[37] B. Jisha, M.R. Resmi, R.J. Maya, R.L. Varma, Tetrahedron Lett. 54 (2013) 4232–4236.
[38] V.P. Singh, K. Tiwari, M. Mishra, N. Srivastava, S. Saha, Sens. Actuators B 182 (2013) 546–554.
[39] E. Kaneko, A. Ishida, Y. Deguchi, T. Yotsuyanagi, Chem. Lett. 23 (1994) 1615–1618.
[40] H. Mizuguchi, E. Kaneko, T. Yotsuyanagi, Analyst 125 (2000) 1667–1671.
[41] X.H. Jiang, B.D. Wang, Z.Y. Yang, Y.C. Liu, T.R. Li, Z.C. Liu, Inorg. Chem. Commun. 14 (2011) 1224–1227.
[42] H.M. Park, B.N. Oh, J.H. Kim, W. Qiong, I.H. Hwang, K.D. Jung, C. Kim, J. Kim, Tetrahedron Lett. 52 (2011) 5581–5584.
[43] Z.C. Liao, Z.Y. Yang, Y. Li, B.D. Wang, Q.X. Zhou, Dyes Pigments 97 (2013) 124–128.
[44] D. Lin-Vien, N.B. Colthup, W.G. Fateley, J.G. Grasselli., The Handbook of Infrared and Raman Characteristic Frequencies of Organic Molecules, Academic Press, Boston, 1991.
[45] E. Pretsch, P. Buhlmann, C. Affolter, Structure Determination of Organic Compounds: Tables of Spectral Data, Springer-Verlag, Berlin Heidelberg, 2000.

[46] K. Nakamoto, Infrared and Raman Spectra of Inorganic and Coordination Compounds, sixth edition, John Wiley & Sons, Inc., New Jersey, 2008.
[47] C. Wyganowski, S. Motomizu, K. Tôei, Anal. Chim. Acta 140 (1982) 313–317.
[48] B. Bouzid, A.M.G. Macdonald, Anal. Chim. Acta 207 (1988) 337–342.
[49] R.L. Benson, P.J. Worsfold, F.W. Sweeting, Anal. Chim. Acta 238 (1990) 177–182.
[50] A. Prownpuntu, U. Titapiwatanakun, Analyst 116 (1991) 191–194.
[51] D.J. Malcolme–Lawes, K.H. Wong, J. Autom. Chem. 13 (1991) 147–151.
[52] M.J. Quintela, M. Gallego, M. Valcárcel, Analyst 118 (1993) 1199–1203.
[53] R.J. Cassella, R.E. Santelli, A.G. Branco, R.J. Cassella, V.A. Lemos, S.L.C. Ferreira, M. Souza de Carvalho, Analyst 124 (1999) 805–808.
[54] Y. Zhou, H. Wang, G. Sun, Y. Fan, X. Chen, Z. Hu, Fresenius J. Anal. Chem. 366 (2000) 17–21.